



This is a repository copy of *Establishing operando diffraction capability through the study of Li-ion (de) intercalation in LiFePO₄*.

White Rose Research Online URL for this paper:
<http://eprints.whiterose.ac.uk/161516/>

Version: Published Version

Proceedings Paper:

Wilson, G., Zilinskaite, S., Unka, S. et al. (2 more authors) (2020) Establishing operando diffraction capability through the study of Li-ion (de) intercalation in LiFePO₄. In: Cruden, A., (ed.) Energy Reports. 4th Annual CDT Conference in Energy Storage & Its Applications, 09-10 Jul 2019, Southampton, UK. Elsevier , pp. 174-179.

<https://doi.org/10.1016/j.egy.2020.03.022>

Reuse

This article is distributed under the terms of the Creative Commons Attribution-NonCommercial-NoDerivs (CC BY-NC-ND) licence. This licence only allows you to download this work and share it with others as long as you credit the authors, but you can't change the article in any way or use it commercially. More information and the full terms of the licence here: <https://creativecommons.org/licenses/>

Takedown

If you consider content in White Rose Research Online to be in breach of UK law, please notify us by emailing eprints@whiterose.ac.uk including the URL of the record and the reason for the withdrawal request.



eprints@whiterose.ac.uk
<https://eprints.whiterose.ac.uk/>



4th Annual CDT Conference in Energy Storage and Its Applications, Professor Andrew Cruden, 2019, 07–19, University of Southampton, UK

Establishing *operando* diffraction capability through the study of Li-ion (de) intercalation in LiFePO₄

George Wilson, Silvija Zilinskaite, Shiv Unka, Rebecca Boston, Nik Reeves-McLaren*

Department of Materials Science and Engineering, University of Sheffield, S1 3JD, UK

Received 18 February 2020; accepted 22 March 2020

Abstract

We have used a laboratory diffractometer to perform *operando* X-ray diffraction on LiFePO₄ during electrochemical cycling in a coin cell fitted with a Kapton window. The results obtained are in good agreement with previous studies, verifying that extraction of Li from LiFePO₄ follows dual-phase solid solution behaviour, with neither LiFePO₄ nor FePO₄ maintaining a static composition during deintercalation.

© 2020 Published by Elsevier Ltd. This is an open access article under the CC BY-NC-ND license (<http://creativecommons.org/licenses/by-nc-nd/4.0/>).

Peer-review under responsibility of the scientific committee of the 4th Annual CDT Conference in Energy Storage and Its Applications, Professor Andrew Cruden, 2019.

Keywords: Energy storage; *Operando* XRD; Lithium iron phosphate; Phase change

1. Introduction

Energy storage devices such as lithium-ion batteries are increasingly ubiquitous in modern society, with wide-ranging applications in consumer electronics, electric and hybrid vehicles, and grid-scale storage for power generated via sustainable resources. Significant issues remain, with many aspects of their long-term use, in for example capacity fading, ageing and cycling performance, still requiring optimisation.

In order to design better batteries, improved understanding of the processes which occur inside individual battery cells during electrochemical (dis)charging is required. Many battery materials are sensitive to air and/or moisture, and would deteriorate or combust if a cell were to be prised open and studied under atmospheric conditions. *Operando* studies offer an ideal solution to this problem, where the ongoing redox and ageing processes can be studied in real time during testing under real working conditions, without requiring cell disassembly.

Traditionally, studies of this nature have been made using neutron or synchrotron radiation available only at large-scale central facilities. While these offer rapid and highly penetrating solutions for *operando* work, accessing the facilities can be difficult and typically involves long delays while research proposals are written and submitted

* Corresponding author.

E-mail addresses: r.boston@sheffield.ac.uk (R. Boston), n.reeves@sheffield.ac.uk (N. Reeves-McLaren).

<https://doi.org/10.1016/j.egy.2020.03.022>

2352-4847/© 2020 Published by Elsevier Ltd. This is an open access article under the CC BY-NC-ND license (<http://creativecommons.org/licenses/by-nc-nd/4.0/>).

Peer-review under responsibility of the scientific committee of the 4th Annual CDT Conference in Energy Storage and Its Applications, Professor Andrew Cruden, 2019.

for peer review in the hope of beamtime being successfully awarded. This process is often time-consuming, with proposals having no guarantee of success.

The use of standard laboratory diffractometers is widespread amongst those studying energy storage materials. Most are fitted with Cu radiation sources, which is poorly penetrating and restricts work to the study of processes inside half-cells only, where the active electrode of interest is cycled vs. a lithium metal foil anode. The low flux of such sources and common use of low-efficiency scintillation counter detectors can make performing experiments in anything like real time very difficult.

Harder radiation laboratory X-ray sources, with *e.g.* Ag radiation, have been available for some time, but until relatively recently their very poor flux made them very much a niche application with experiment times measured in days or weeks. In recent years, however, detectors, *e.g.* PANalytical's GaliPIX and Bruker's LynxEye XE, have been able to offer ~100% efficiency with hard radiations and has opened up the market for performing *operando* studies in close to real time, with half and pouch cells in laboratory settings [1].

In this study, we share the results of a preliminary *operando* study on lithium iron phosphate, LiFePO₄, which has been well studied over the past 20 years [2–6]. Initially showing poor electrochemical performance, commercialisation has been realised largely through a combination of (i) development of surface coating and doping strategies, to improve its electronic conductivity [7–10], and (ii) nano-scaling [11], to reduce the length of Li⁺-ion diffusion pathways [12].

There has been much debate, however, on the processes that occur during the extraction and insertion of Li⁺-ions during (de)intercalation, and how these might vary with charge rate as manufacturers and consumers seek ever faster charging capabilities. A number of mechanisms have been proposed, based on *e.g.* core-shell, shrinking core and domino-cascade models [13–15]. These models have often been based on findings from *ex situ* techniques, including XRD; *operando* studies that monitor processes occurring during real-time Li (de)intercalation have, until recently, been few and far between.

One such study was made by Liu *et al.* in 2014 [16], which used a synchrotron radiation source to show that a dual-phase solid solution mechanism exists for LiFePO₄; as Li is extracted, both Li-rich Li_{1-x}FePO₄ and Li-poor Li_yFePO₄ phases coexist for much of the (dis)charge processes. However, at the start and end of (dis)charging, both the LiFePO₄ and FePO₄ exhibit solid-solution type behaviour.

At the University of Sheffield, the home department of the authors of this current study has recently procured a new hard-radiation diffractometer. Fitted with Ag radiation and a GaliPIX detector, this instrument is ideally suited for *operando* studies. Here, we present the preliminary findings of our first such study, using LiFePO₄ as a model compound and to verify the existence of this dual-phase solid solution mechanism in LiFePO₄, with our readily-accessible laboratory diffractometer.

2. Experimental

For this study, the active material selected was as received lithium iron phosphate (LiFePO₄ or LFP, >97% purity, Sigma Aldrich). Phase was verified by X-ray diffraction using a Bruker D2 Phaser, with Ni-filtered Cu-K α radiation ($\lambda = 1.5406 \text{ \AA}$) and a LynxEye^{1D} detector. Analyses were conducted using the International Centre for Diffraction Data's PDF-4+ database (2019 edition) and SLeve+ software.

Electrodes were prepared by mixing the active material (LiFePO₄), PVdF binder and carbon (Super C65, Imerys Graphite & Carbon) in a weight ratio of 95:2.5:2.5 respectively, and dispersing in a sufficient volume of 1-methyl-2-pyrrolidone (anhydrous 99.5%, Sigma Aldrich). The resulting slurry was centrifuged for 30 min, then cast onto battery grade carbon-coated Al foil using a micrometer adjustable blade applicator. The sheets were dried under vacuum, then calendared using a rolling mill to give a coating thickness of *ca.* 70 μm , and 12 mm diameter discs punched for use in electrochemical testing.

Stainless steel 2016-type coin cells were assembled in an argon-filled glovebox (MBraun) for standard electrochemical cycling. Cells were constructed by layering a stainless steel spacer, a freshly cut and cleaned Li metal disk as the counter electrode, a glass fibre separator (GF/F, Whatman) soaked in 1 M LiPF₆ in ethylene carbonate/dimethyl carbonate (EC/DMC, 1:1, v/v) (Sigma Aldrich), and then a disk of the cathode under study.

Electrochemical tests were performed on these 2016 coin cells in climatic chambers at 25 °C and cells were left to rest at open circuit conditions for 8 h before cycling, before being cycled galvanostatically between 2.0–4.5 V vs. Li/Li⁺ at a rate of 0.1 C (17 mA g⁻¹) using a Maccor Series 4000 Battery Cycler. Electrochemical testing was

performed on four cells to ensure reproducibility. All subsequent references to potential and voltage are relative to the Li/Li^+ reference.

For *operando* cycling, cells were constructed as above but using adapted coin cells (MTI), fitted with a 10 mm Kapton window in the positive-end casing to allow penetration by X-rays. These cells were allowed to rest for 8 h, and then mounted into a proprietary coin cell holder (Malvern Panalytical). *Operando* cells were cycled galvanostatically between 2–4.5 V for one charge–discharge loop at a rate of 0.1 C using a Maccor Series 4300 Battery Cycler. During this cycling, XRD data were collected continuously using a PANalytical Empyrean diffractometer, with Rh-filtered $\text{Ag K}\alpha$ radiation ($\lambda = 0.5594 \text{ \AA}$) and a GaliPIX detector with CdTe sensor allowing *ca.* 100% efficiency for hard radiation. Each diffraction dataset took a total of 8 min to collect, with a subsequent 2-min dwell to allow time for data recording, opening and closing of X-ray shutters *etc.*

3. Results and discussion

X-ray diffraction data as shown in Fig. 1 for the as-received LiFePO_4 showed excellent agreement against reference data from the ICDD database, PDF card number 00-040-1499 [17]. No additional Bragg reflections were observed, with all peaks indexed to the expected $Pnma$ space group; the material can therefore be assumed to be single phase.

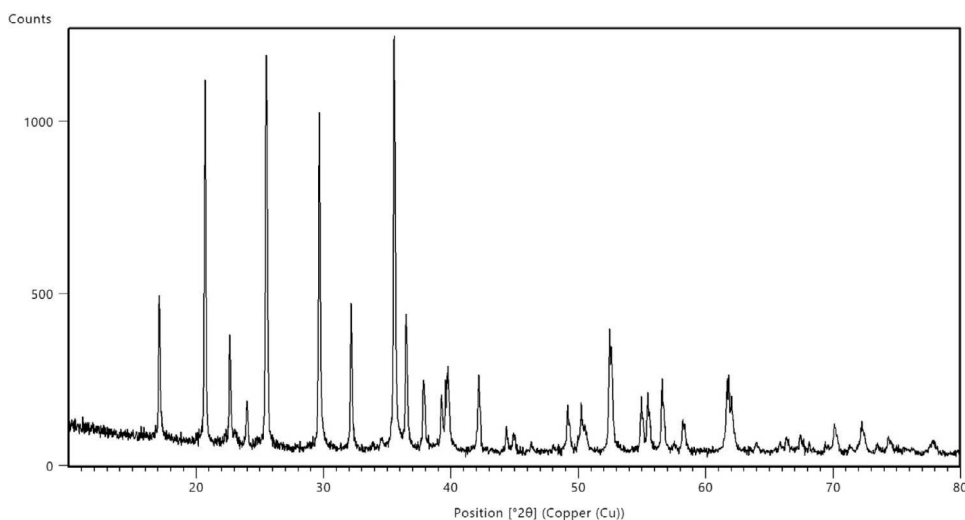


Fig. 1. Powder X-ray diffraction data for as-received LiFePO_4 .

Standard coin cells containing LiFePO_4 were tested over 20 charge–discharge cycles, with first cycle discharge capacities of 139 mA h g^{-1} , centred on a plateau at *ca.* 3.4 V, Fig. 2. This represents 82% of the theoretical maximum of 170 mA h g^{-1} . On further cycling, the cell cycles with excellent reversibility with a discharge capacity of *ca.* 135 mA h g^{-1} still retained after 20 cycles, as shown in Fig. 3.

The electrochemical data, Fig. 4a, for the *operando* cell with Kapton window cycled once inside the diffractometer are broadly very similar. After the initial rest period, the charge profile shows a rapid increase in potential to a single broad plateau centred at *ca.* 3.5 V. On subsequent discharging, the plateau is observed with a slight hysteresis at *ca.* 3.3 V; the observed discharge capacity was marginally higher for this cell, relative to the standard 2016 cells, at 149 mA h g^{-1} , but no checks have been made on the reproducibility of this to date.

Diffraction data for the full charge–discharge profile are presented in Fig. 4b; detailed XRD patterns for a narrower range from 10 to $15^\circ 2\theta$ are shown in Fig. 5. In the full profiles, some Bragg peaks can be seen to remain constant regardless of cell (dis)charge state; these can be indexed to the carbon black (at $9^\circ 2\theta$), the aluminium current collector (at 15.8 and $22.5^\circ 2\theta$), and the steel casing of the coin cell (at 15.4 and $17.8^\circ 2\theta$). These peaks will not be discussed further, though they are always present; all other observed Bragg reflections can be indexed to LiFePO_4 and/or FePO_4 , dependent on the state of charge.

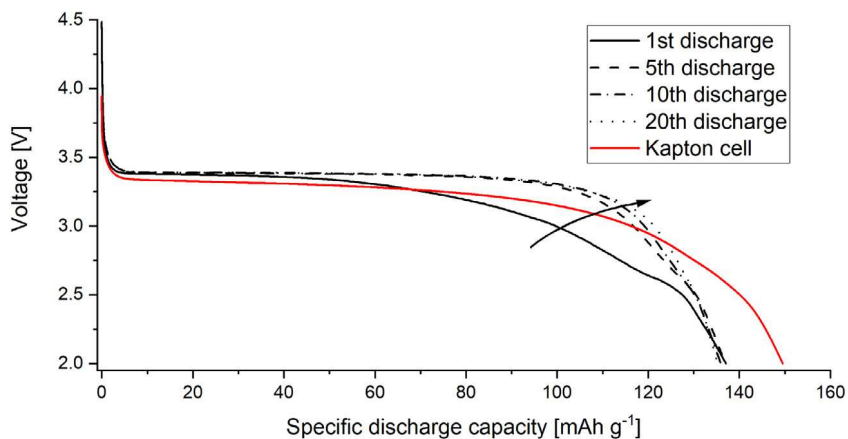


Fig. 2. Voltage profile of the first 20 discharge cycles of a standard LiFePO_4 cell at 17 mA g^{-1} in the voltage range of 2.0 V and 4.5 V, and the first discharge cycle of a LiFePO_4 cell with a Kapton window at 17 mA g^{-1} in the voltage range of 2.0 V to 3.95 V. The arrow indicates increasing cycle number for the standard coin cell.

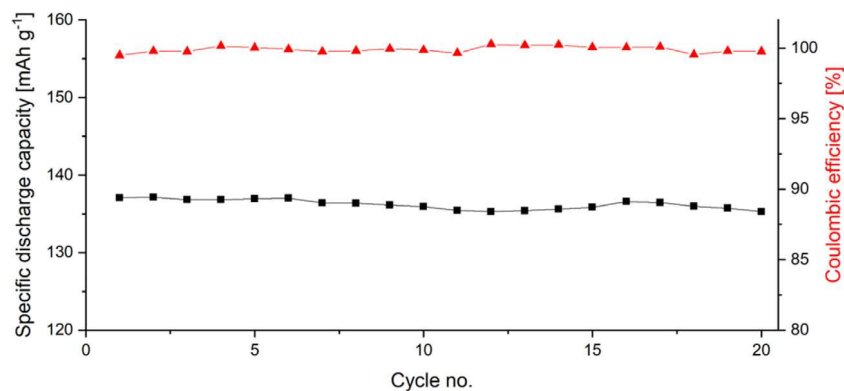


Fig. 3. Specific discharge capacity and coulombic efficiency for a standard LiFePO_4 cell at 17 mA g^{-1} in the voltage range of 2.0 V and 4.5 V.

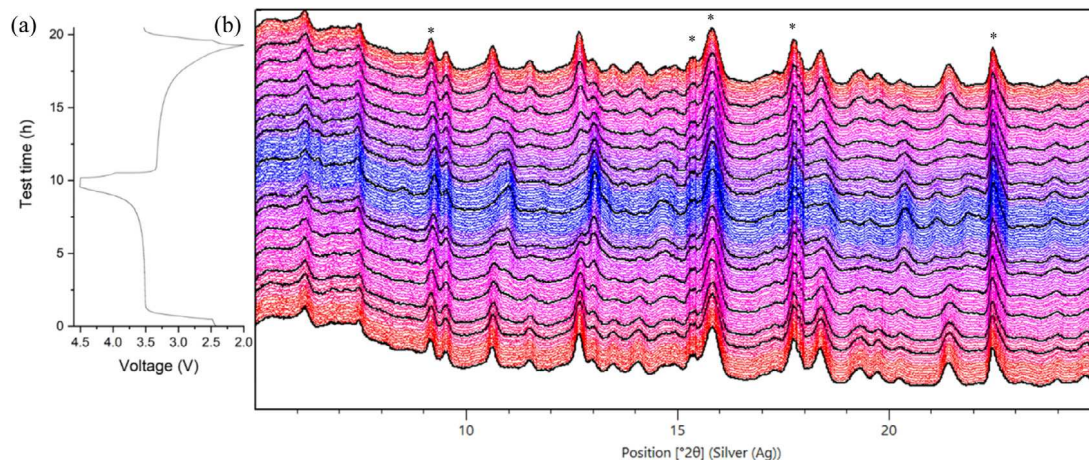


Fig. 4. (a) The voltage profile of LiFePO_4 during first charge and discharge, and (b) the XRD patterns of the Kapton cell over the first charge and discharge. All peaks corresponding to inactive material are marked *.

It should be noted that since LiFePO_4 and FePO_4 both crystallise in the same $Pnma$ space group, the diffraction patterns are very similar; however, there are significant differences in the lattice parameters for the two phases, and so the characteristic peaks from LiFePO_4 and FePO_4 can be easily distinguished.

During the rest period before cycling, the diffraction data from the *operando* cell show only the Bragg reflections from LiFePO_4 , as expected. With the onset of charging, the peaks for LiFePO_4 move to higher scattering angles, indicating a contraction in the unit cell size as Li is extracted from the material [18]. This is well evidenced by the intense 311 reflection in Fig. 5. Initially, however, no additional reflections are observed, showing that, at least in this study, a single-phase region exists at the beginning of the charging process, where the active material takes the form $\text{Li}_{1-x}\text{FePO}_4$.

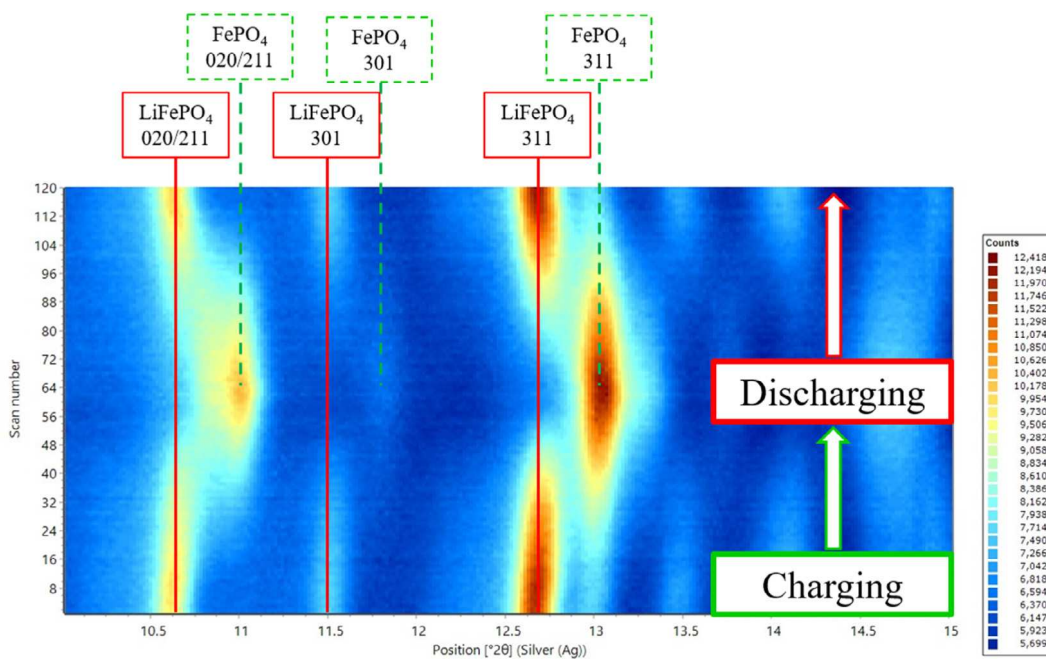


Fig. 5. Contour plot of diffraction peak intensities for selected Bragg reflections for LiFePO_4 and FePO_4 during first charge–discharge cycle.

The emergence of the FePO_4 phase becomes apparent from the appearance of its (020) reflection at $\sim 11^\circ 2\theta$ in diffraction data with the cell having reached a potential of *ca.* 3.51 V (Fig. 5). Peaks from both LiFePO_4 and FePO_4 are apparent at this stage as charging continues to a potential of *ca.* 4.08 V, indicating that both are coexistent over this range. Thereafter, only the peaks from FePO_4 are observed until charging ends when the cell attains 4.5 V; again, these peaks show a very slight deviation to higher scattering angles as charging proceeds — for example, the (430) reflection, not shown, moves from $20.34^\circ 2\theta$ with the cell at \sim to $20.38^\circ 2\theta$ when the cell reaches 4.5 V. Although a minor shift, this suggests again that the composition of FePO_4 is varying as Li deintercalation is reaching its conclusion.

On discharge, the reverse behaviour is seen, with peaks FePO_4 returning to lower scattering angles during discharge, and peaks for LiFePO_4 quickly reappearing as the cell potential reaches ~ 3.5 V. Peaks for FePO_4 gradually shrink, and can no longer be resolved from the background once the cell has been discharged to ~ 3.05 V.

4. Conclusion

The changes observed indicate the coexistence of both LiFePO_4 and FePO_4 throughout the majority of the (dis)charging processes, but that single phase regions exist at both low and high states of charge. The shifting of peaks observed shows that solid solution reaction mechanisms exist in both of these single-phase regions, with a Li-rich $\text{Li}_{1-x}\text{FePO}_4$ phase present as charging commences, and a single Li-deficient Li_yFePO_4 phase existing towards the end of the charge process. These results are consistent with the ‘dual-phase solid solution’ model proposed by Liu *et al.* [16] for Li-ion (de)intercalation in LiFePO_4 . However, while previous reports have used synchrotron

X-radiation to perform *operando* experiments and observe this behaviour in real-time, here we have demonstrated that the same is possible using a much-more readily accessible laboratory source.

Declaration of competing interest

The authors declare that they have no known competing financial interests or personal relationships that could have appeared to influence the work reported in this paper.

Acknowledgements

GW acknowledges support from the Centre for Doctoral Training in Energy Storage and its Applications from the EPSRC. We wish to acknowledge the Henry Royce Institute for Advanced Materials (EPSRC, United Kingdom Grant Number EP/R00661X/1) for the PANalytical Empyrean access at Royce@Sheffield. RB acknowledges that this project was supported by the Lloyd's Register Foundation, United Kingdom and Royal Academy of Engineering, United Kingdom under the Research Fellowship scheme. SZ acknowledges support from the Lloyd's Register Foundation, a charitable foundation, helping to protect life and property by supporting engineering-related education, public engagement and the application of research through the International Consortium in Nanotechnology (ICON) hosted by the University of Southampton.

References

- [1] Kim H, Kim JC, Bo SH, Shi T, Kwon DH, Ceder G. K-ion batteries based on a P2-type $K_{0.6}CoO_2$ cathode. *Adv Energy Mater* 2017;7(17):2–7.
- [2] Yamada A, Chung SC, Hinokuma K. Optimized $LiFePO_4$ for lithium battery cathodes. *J Electrochem Soc* 2001;148(3):A224.
- [3] Wang D, Li H, Shi S, Huang X, Chen L. Improving the rate performance of $LiFePO_4$ by Fe-site doping. *Electrochim Acta* 2005;50(14):2955–8.
- [4] Delacourt C, Poizot P, Levasseur S, Masquelier C. Size effects on carbon-free $LiFePO_4$ powders. *Electrochem Solid-State Lett* 2006;9(7):A352.
- [5] Doughty DH, Roth EP. A general discussion of Li ion battery safety. *Interface Mag* 2016;21(2):37–44.
- [6] Su W, Xu K, Zhong G, Wei Z, Wang C, Meng Y. Enhanced electrochemical performance of $LiFePO_4$ as cathode for lithium ion battery by codoping with titanium and nitrogen. *Int J Electrochem Sci* 2017;12(8):6930–9.
- [7] Chung SY, Bloking JT, Chiang YM. Electronically conductive phospho-olivines as lithium storage electrodes. *Nature Mater* 2002;1(2):123–8.
- [8] Shi S, Liu L, Ouyang C, Wang D, Wang Z, Chen L, et al. Enhancement of electronic conductivity of $LiFePO_4$ by Cr doping and its identification by first-principles calculations. *Phys Rev B* 2003;68(19):1–5.
- [9] Mi CH, Zhao XB, Cao GS, Tu JP. In situ synthesis and properties of carbon-coated $LiFePO_4$ as li-ion battery cathodes. *J Electrochem Soc* 2005;152(3):A483.
- [10] Sides CR, Croce F, Young VY, Martin CR, Scrosati B. A high-rate, nanocomposite $LiFePO_4$ /carbon cathode. *Electrochem Solid State Lett* 2005;8(9):A484–7.
- [11] Armand M, Gauthier M, Magnan J, Ravet N. Method for synthesis of carbon-coated redox materials with controlled size. 2001;1:83.
- [12] Wu X-L, Jiang L-Y, Cao F-F, Guo Y-G, Wan L-J. $LiFePO_4$ nanoparticles embedded in a nanoporous carbon matrix: Superior cathode material for electrochemical energy-storage devices. *Adv Mater* 2009;21(25–26):2710–4.
- [13] Padhi AK, Nanjundaswamy KS, Goodenough JB. Phospho-olivines as positive-electrode for rechargeable lithium batteries. *J Electrochem Soc* 1997;144(4):1188–94.
- [14] Andersson AS, Thomas JO. The source of first-cycle capacity loss in $LiFePO_4$. *J Power Sources* 2001;97(98):498–502.
- [15] Delmas C, Maccario M, Croguennec L, Cras FLe, Weill F. Lithium deintercalation in $LiFePO_4$ nanoparticles via a domino-cascade model. *Nature Mater* 2008;7(8):665–71.
- [16] Liu Q, He H, Li ZF, Liu Y, Ren Y, Lu W, et al. Rate-dependent, Li-ion insertion/deinsertion behavior of $LiFePO_4$ cathodes in commercial 18650 $LiFePO_4$ cells. *ACS Appl Mater Interfaces* 2014;6(5):3282–9.
- [17] Kabekkodu S. ICDD 2019. PDF-4 2019 (Database). Newtown Square; 2019.
- [18] Han SC, Lim H, Jeong J, Ahn D, Park WB, Sohn KS, et al. Ca-doped Na_xCoO_2 for improved cyclability in sodium ion batteries. *J Power Sources* 2015;277:9–16.